Australian Journal of Basic and Applied Sciences, 3(4): 3757-3770, 2009
ISSN 1991-8178

A Geometrical Motion Planning Approach For Redundant Planar Manipulators

[1]Samer Yahya, [2]Haider A. F. Mohamed, Member, *IEEE,* [1]M. Moghavvemi, Member, *IEEE*

[1]Center of Research in Applied Electronics (CRAE) University of Malaya, 50603 Kuala Lumpur, Malaysia
[2]Department of Electrical & Electronic EngineeringThe University of Nottingham Malaysia CampusJalan Broga, 43500 Semenyih, Selangor Darul Ehsan, Malaysia

Abstract: Efficient control of industrial robots is an important factor in the success of industrial automation. Motion planning of robot manipulators is one of the challenging problems encountered in this field. This paper proposes a method for the motion planning of the redundant planar manipulators. The main idea is to find a smooth path consisting of points close enough to each other and geometrically compute their inverse kinematics. The proposed method will generate a single solution. Which makes the problem of finding one solution among the infinite solutions caused by redundancy is avoided. To demonstrate the effectiveness of the proposed method, this paper considers a 5-links redundant manipulator, the results are very promising.

Key words: Motion-Planning, Redundancy, Manipulators-Kinematics.

INTRODUCTION

A manipulator with more degrees of freedom than necessary is called kinematically a redundant manipulator (Mittal and Nagrath, 2007; Gianluca, 2008; Damir Omrcen, *et al.,* 2007). It is expected that the manipulator with redundancy brings sophisticated motion that makes it possible to realize a flexible motion according to environmental changes (Shibata and Murakami, 2007). Redundant degrees of freedom means there are multiple ways of moving the joints that will accomplish the same motion (Robin, 2000).

Usually, kinematics of non redundant robots is solved by deriving analytical solutions for several manipulator configurations. The analytical solutions offer minimal numerical complexity, together with special treatment of singularities (Kircanski and Petrovic,1991). When a manipulator is redundant, it is anticipated that the inverse kinematics admits an infinite number of solutions. This implies that, for a given location of the manipulator's end-effecter, it is possible to induce a self-motion of the structure without changing the location of the end-effecter (Maria *et al.,* 2008). Therefore, the classical methods cannot be used for solving their inverse kinematics.

Generally, there are many algorithms for the redundant manipulator inverse kinematics. These algorithms can be divided into three categories (Sheng *et al.,* 2006). 1. the algebraic approach (Perez and McCarthy, 2005). 2. the iterative approach, such as neural networks (Xia and Wang, 2001). genetics algorithm (Nearchou, 1998). and fuzzy logic (Naoyuki Kubota, 1998). and 3. the geometric approach (Sheng *et al.,* 2006; Bayraktaroglu *et al.,* 1999; Lee and Ziegler, 1984).

The algebraic approach suffers from the fact that it does not give a clear indication on how to select the correct solution from the several possible solutions for a particular arm configuration. The user often needs to rely on his/her intuition to pick the right answer. The iteration solution does not guarantee convergence to the correct solution. Furthermore, just like the algebraic approach there is no indication of how to choose the correct solution for a particular arm configuration. The geometrical approach on the other hand can provide the solution directly with simple calculations.

This paper proposes a geometrical method that can be used to find one solution for the inverse kinematics of planar redundant manipulators. Also the result of the proposed method is compared with the result in [8] to show the validity of the proposed method, and it will be noted that the proposed method can be used to improve the manipulability compared with the result in (Sheng *et al.,* 2006).

Corresponding Author: Samer Yahya, Center of Research in Applied Electronics (CRAE) University of Malaya, 50603 Kuala Lumpur, Malaysia
E-mal: haider.abbas @nottingham.edu.my

The Geometrical Method of the Inverse Kinematics:

Consider the n DOF manipulator shown in Fig. 1 whose joint variables are denoted by: $q= [q_1,q_2,\ldots, q_n]$, where qi denotes the i-th joint variable, ji denotes the i-th joint, and li denotes length of the i-th link. To explain the proposed method, the following steps are to be followed considering that tp is the target point:

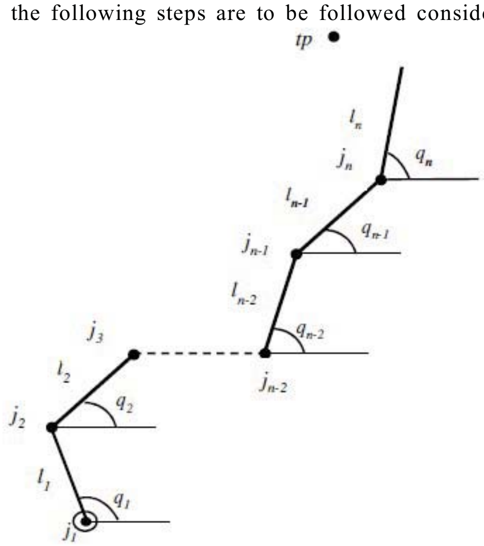

Fig.1: A planar maninpulator with n links.

1.Draw a circle with a radius equal to the length of the last link and the center of this circle is at the target point tp. The circle equation is:

$$(x- xtp\ )^{2+y-}\ (ytp\ )2=l_n^2 \tag{1}$$

2.Draw a straight line from the center of this circle to the joint jn, Fig. 2 shows these steps. Now the end-effecter at the target point tp and the other end (the new joint jn') is at the intersection point between the circle and the straight line. Therefore, the joint angle of the last link qn is found. The straight line equation in this case is:

$$x(\ y_{jn}\ -y_{tp})+y(x_{tp}\ -x_{jn}\ )=x_{tp}\ y_{jn}\ -y_{tp}\ x^{jn} \tag{2}$$

From (1) and (2) there are two intersection points. The nearer point to the joint jn should be selected. The coordinates of the intersection points are:

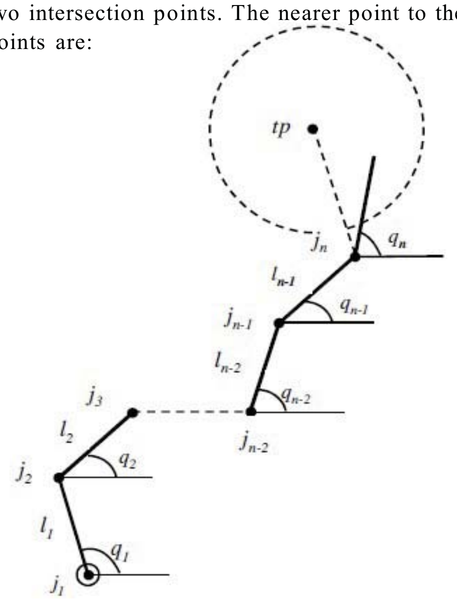

Fig. 2: Steps (1) and (2).

$$x'_{jn} = \frac{-b \pm \sqrt{b^2 - 4ac}}{2a} \tag{3}$$

$$y'_{jn} = \frac{x_{tp}y_{jn} - y_{tp}x_{jn}}{\partial u \partial v} - x'_{jn}\left(\frac{y_{jn} - y_{tp}}{x_{tp} - x_{jn}}\right) \tag{4}$$

Now, the new position of last link can be obtained, where:

$$a = 1 + \left(\frac{y_{jn} - y_{tp}}{x_{tp} - x_{jn}}\right)^2 \tag{5}$$

$$b = -2x_{tp} - 2\frac{y_{jn}y_{tp}}{x_{tp} - x_{jn}}\left(\frac{x_{tp}y_{jn} - y_{tp}x_{jn}}{x_{tp} - x_{jn}} - y_{tp}\right) \tag{6}$$

$$c = x_{tp}^2 + \left(\frac{x_{tp}y_{jn} - y_{tp}x_{jn}}{x_{tp} - x_{jn}} - y_{tp}\right)^2 - l_n^2 \tag{7}$$

3.A new circle with the radius of the next link length i.e. l_{n-1} is drawn, its center is at the new joint *jn’*, Fig. 3. shows this step. The circle equation is:

$$(x - x'_{jn})^2 + (y - y'_{jn})^2 = l_{n-1}^{\;2} \tag{8}$$

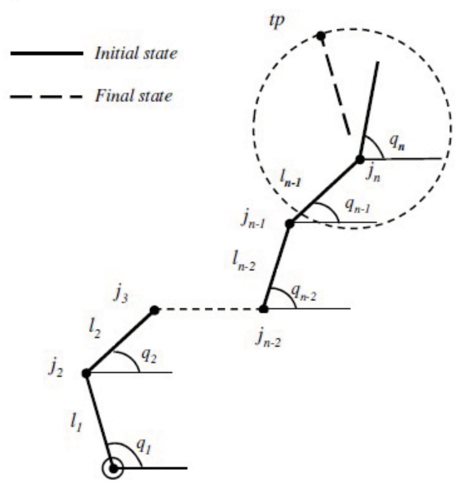

Fig. 3: Step (3).

4.The next step is to draw another straight line from the center of the last circle to the joint $_{jn-1,}$ Now get the new position of the link $_{ln-1,}$ where the tip of this link is at the center of the last circle, and the other end (the new joint $_{jn-1'}$) is at the intersection between this circle and the straight line as shown in Figs. 4. and 5. Therefore, the joint angle of the link $_{qn-1}$ is found. The straight line equation is:

$$x(y_{jn} - y'_{jn}) + y(x'_{jn} - x_{jn-1}) = x'_{jn}y_{jn-1} - y'_{jn}x_{jn-1} \tag{9}$$

There are two intersection points; the nearer point to the joint $_{jn-1}$ is selected. The coordinates of the intersection points are:

$$x'_{jn} = \frac{-b \pm \sqrt{b^2 - 4ac}}{2a} \tag{10}$$

$$y'_{jn} = \frac{x'_{jn}y_{jn-1} - y'_{jn}x_{jn.1}}{x'_{jn} - x_{jn-1}} - x'_{jn-1}\left(\frac{y_{jn-1} - y'_{jn}}{x'_{jn} - x_{jn-1}}\right) \tag{11}$$

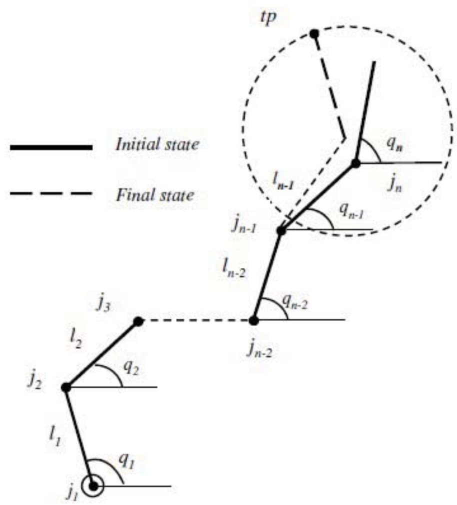

Fig. 4: Finding the new state of the link l_{n-1}.

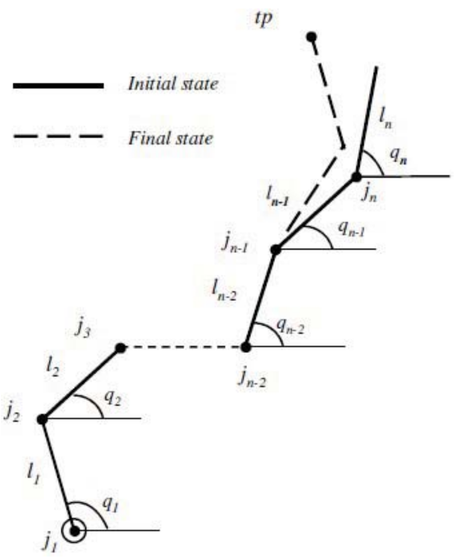

Fig. 5: The new state of the link l_{n-1}.

where:

$$a=1+\left(\frac{y_{jn}-y'_{jn}}{x'_{jn}-x'_{jn-1}}\right)^2 \tag{12}$$

$$b=-2x'_{jn}-2\frac{y'_{jn-1}-y'_{jn}}{x'_{jn}-x_{jn-1}}\left(\frac{x'_{jn}y_{jn-1}-y'_{jn}x_{jn-1}}{x'_{jn}-x_{jn-1}}-y'_{jn}\right) \tag{13}$$

$$c=x'^{\,2}_{jn}+\left(\frac{x'_{jn}y_{jn-1}-y'_{jn}x_{jn-1}}{x'_{jn}-x_{jn-1}}-y'_{jn}\right)-l_{n-1}^{\,2} \tag{14}$$

5.Find the new state for the other links by the same way until reaching the new joint j_3'.

6.To find the new state of the first two links, two circles should be drawn, the radius of the first circle is equal to the length of the first link and the radius of the second circle is equal to the length of the second link. The center of the first one is at the origin point *j1* and the center of the second circle is at the new joint j_3' as shown in Fig. 6. The circles equations are:

$$x^2 + y^2 = l_1^2 \tag{15}$$

$$(x - x'_{j3})^2 + (y - y'_{j3})^2 = l_2^3 \tag{16}$$

The coordinates of the intersection points between the circles are:

$$x'_{j2} = \frac{-b \pm \sqrt{b^2 - 4ac}}{2a} \tag{17}$$

$$y'_{j2} = \pm\sqrt{l_1^2 - x'^2_{j2}} \tag{18}$$

where:

$$a = 1 + (\frac{x'_{j3}}{y'_{j3}})^2 \tag{19}$$

$$c = (\frac{x'^2_{j3} + y_{j3}^2 + l_j^2 - l_2^2}{x'_{jn} - x_{jn-1}})^2 - l_1^2 \tag{20}$$

7. Draw a straight line from the new joint j_3' to the intersection point of the two circles (the new joint *j^2')*, this straight line represents the new position of the second link. By the same way the straight line between the intersection of the two circles and the origin point j_1 represents the new position of the first link. It is noted that there are two possible states for these two links, because there are two intersection points between the circles. Fig. 7 illustrates these possible positions.
8. Select the intersection point which is nearer to the current joint j_2 as a new joint j_2'. Fig. 8. illustrates the initial and final states of the manipulator.

After implementing these steps, the new state of the links will be calculated, except there is a special case, when the intersection point between the circle and the straight line is out of the reachable area of the current joint.

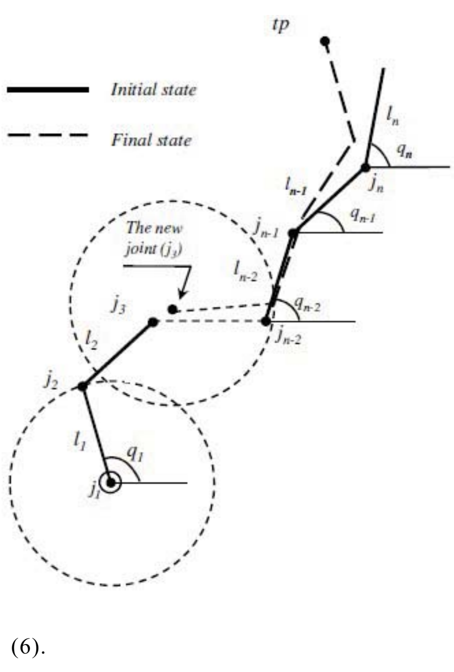

Fig. 6: The two circles of step (6).

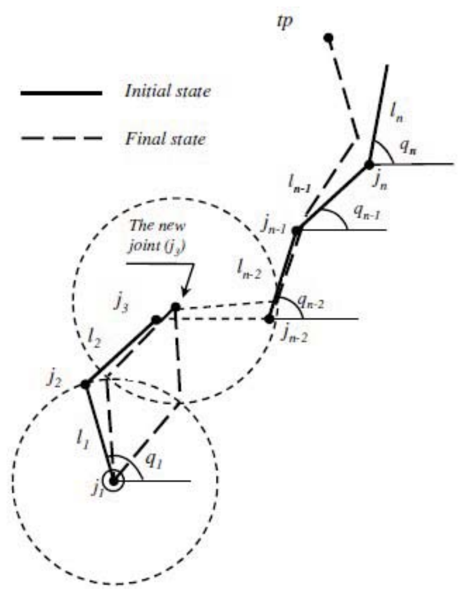

Fig. 7: The two possible positions of the first two links.

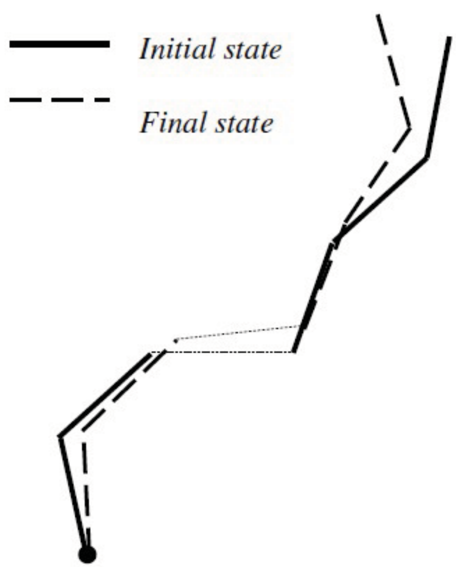

Fig. 8: The initial and expectative states of the manipulator.

9.When the new position of any joint (*i*-th joint) is specified by finding the intersection point of the circle and the straight line as explained previously, if

$$x_i^2 + y_i^2 \rangle \sum_{j=1}^{i-1} l_j^2 \tag{22}$$

this indicates that the intersection point is out of the reachable area of the *i*-th joint, where *xi* and *yi* are the *x*-axis and *y*-axis of the intersection point. In this case another circle must be drawn, the center of which is at the origin *j1* and the radius is equal to the reachable area of the *i*-th joint.

To further explain this case, the following example based on Fig. 9. is considered. To find the new position of joint *jn,* a circle should be drawn, its center is at the target point *tp* and the radius of this circle is equal to the last link length. Then a straight line should be drawn from the target point *tp* to the joint *jn*. The intersection point (A) between them is the new position of the joint *jn*. Now if the distance between this new joint which is presented by (A) and the origin *j1* is more than $(l_1+l_2+\ldots+l_n\text{-}1)$, this means that the point (A) is out of the reachable area of the joint *jn*. Therefore, the circle (CR) is drawn with the center at the origin point *j1* and the radius of the circle is equal to $(l_1+l^2+\ldots+l_n\text{-}1)$. One of the intersection points (B) and (C) between the two circles will be the new position of the joint j_n. The nearer one of the points (B) or (C) to the current position of the joint *jn* is the new position of the joint *jn*. In this example, (B) is the new position of the joint j_n.

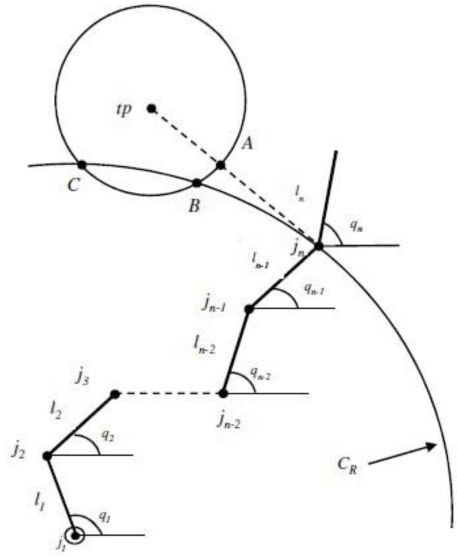

Fig. 9: Special case.

Motion Planning:

The basic idea for motion planning is to find a smooth path consisting of points close enough to each other using the proposed method. Then, using the proposed method to find the inverse kinematics of the manipulator when moving the end-effecter on these path points until the manipulator reaches the target point. To summarize this algorithm, the flow chart depicted in Fig. 10. is constructed. By following these steps, as in the flow chart, the motion planning of the manipulator from the initial point to the target point can be defined.

Firstly the joint variables of the link are given; it is easy to calculate the position of the initial point. To determine the path that the manipulator should follow from the initial point to the target point, the equation

$$y= a+bx \tag{23}$$

is used in this paper. The value of b is known depending on the desired path. The x-axis of the target point is known too. It must be noticed that the value of a and the y-axis of the target point can be easily calculated from the equation above.

From this equation, the path of the end-effecter from the initial point to the target point can be plotted. After calculating the length of this path, a specific number of equally distanced points are plotted on this path. Then, each one of these points is treated as the new target point with respect to the end effecter at the initial position, and not as a target point to the previous point as in reference (Sherg *et al.,* 2006). This means that the inverse kinematics of each point can be calculated using the geometrical approach presented in this paper. By the same way, the inverse kinematics of all points are calculated.

The manipulability is calculated for the result gotten by the proposed method also for the result gotten by using the method in (Sherg *et al.,* 2006). to show the validity of the proposed method.

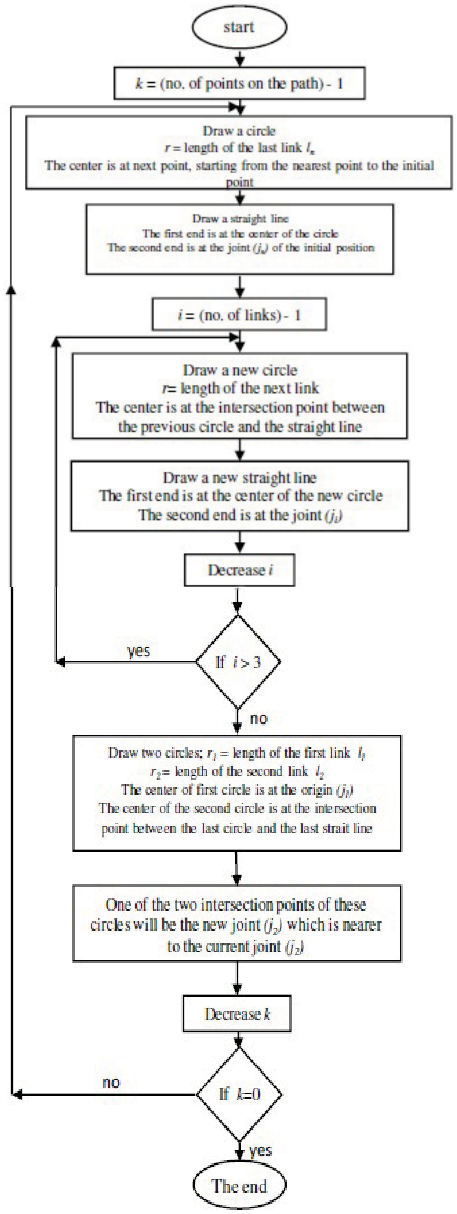

Fig.10: The flowchart of proposed motion planning.

Manipulability Measure:

Manipulability is the ability of robotic mechanisms in positioning and orienting the end-effectors. The manipulability of a robot is not constant, but it varies as a function of the manipulator configuration (Yoshikawa, 1985).

The manipulability is used in this paper to show the effectiveness of the proposed method. The tool position of a two-dimensional planar manipulator is represented by the pair *(x,y),* the joint number *i* varies from 1 to *n, qi* is the angle of the *i* joint, and *li* is the length of the *i*-th link.

$$x = l_1 \cos(q_1)+l_2 \cos(q_2)+....+ l_n \cos(q_n) \tag{24}$$

$$y= l_1\sin(q_1)+l_2\sin(q_2)+....+l_n \sin(q_n) \tag{25}$$

The manipulability measure m of manipulator is based in the Jacobian matrix J, and the Jacobian matrix of the manipulator (Craig, 1989), is given by:

$$j = \begin{bmatrix} \frac{\partial x}{\partial q_1} \frac{\partial x}{\partial q_2} \cdots \frac{\partial x}{\partial q_n} \\ \frac{\partial y}{\partial q_1} \frac{\partial y}{\partial q_2} \cdots \frac{\partial y}{\partial q_n} \end{bmatrix} \tag{26}$$

$$= \begin{bmatrix} -l_1 \sin(q_1) - l_2 \sin(q_2) \ldots - l_n \sin(q_n) \\ -l_1 \cos(q_1) \;\; l_2 \cos(q_2) \ldots l_n \cos(q_n) \end{bmatrix}$$

Then the manipulability measure m of manipulator can be calculated (Allan de *et al.,* 2006):

$$m = \sqrt{\det \left| jj^t \right|} \tag{27}$$

This measure depends of the manipulator configuration and tells us how much freedom the configuration has. Larger values of m means large freedom while small values are normally related to restrictions in the manipulator movements.

To further clarify the proposed method, a 5-links planar manipulator is considered in the next section.

RESULTSAND DISCUSSION

To demonstrate the proposed method, the following 5-links planar manipulator path planning is carried out and simulated. Let l_1=4, l_2=3.5, l_3=3, l_4=2.5, l_5= 2 where the lengths are in units length. The initial state of every joint is given as q=[150°,90°,80°,60°,40°]. The value of the constant b for the equation y=a+bx is b=-1. The x-axis of the target point is 3 units length.

From these given data, the x-axis of the initial point is -0.1611 units length, the y-axis of the initial point is 11.9051 units length, the y-axis of the target point is 8.7440 units length, and the value of a is 11.7440. Fig. 11 illustrates the initial position of the manipulator.

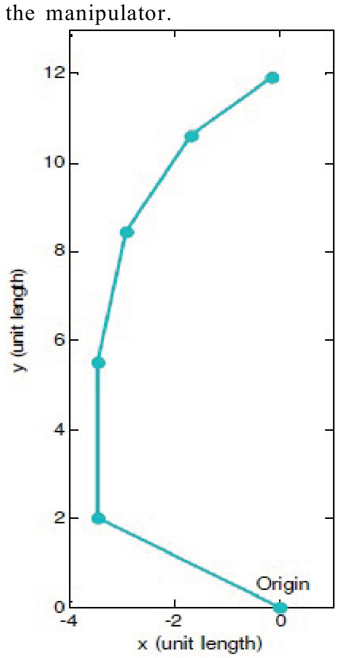

Fig.11: The initial position of the end effecter.

The path that the manipulator must follow from the initial point to the target point is shown in Fig. 12. This figure illustrates also the points that the end effecter should follow to reach the target point. Using the proposed method, the position of next point is shown in Fig. 13.

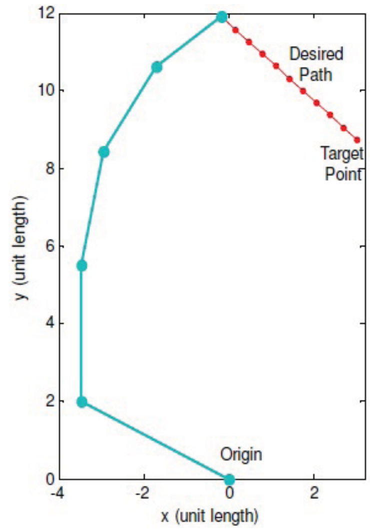

Fig. 12: The initial position of the end effecter and the desired path.

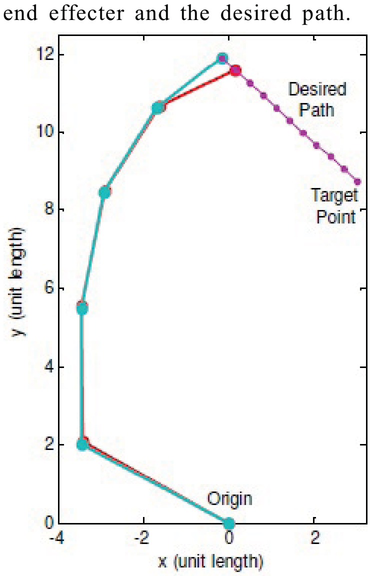

Fig. 13: The initial and second positions of the manipulator.

Then each one of the other points is treated as a new target point with respect to the end effecter at the initial position, Fig. 14 illustrates the motion planning of the manipulator.

Fig. 15 illustrates the motion planning of the manipulator by using the method of reference (Sheng *et al.,* 2006). It is clear that the last link is very close to the desired path which makes the manipulator at this situation less effective in using the last link because the manipulability by using this method is smaller than the value of manipulability by using the proposed method.

The manipulability is calculated for all the manipulator configurations by using the proposed method, and then the manipulability is calculated for all the manipulator configurations by using the method in (Sheng *et al.,* 2006), to show the validity of the proposed method.

Firstly, the positions of all the joints by using the proposed method are given in Tables 1. and 2. From these tables, the angles of the links can be calculated for the manipulator on all the points on the desired path, where:

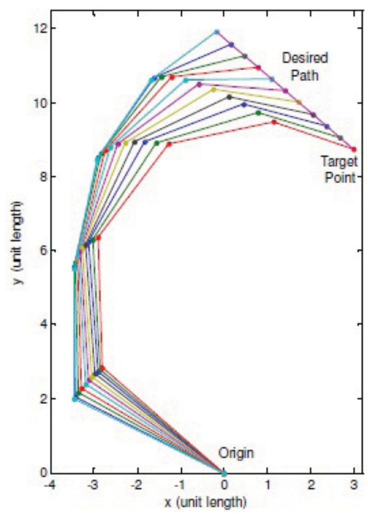

Fig. 14: The motion planning of the manipulator.

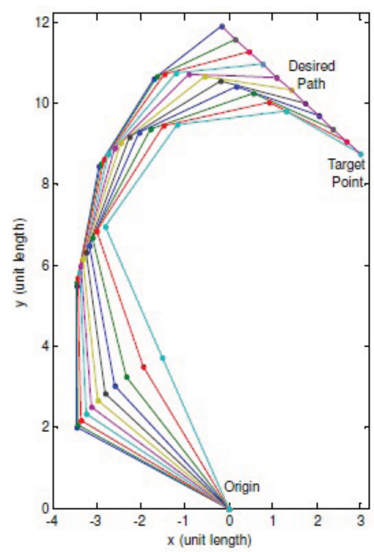

Fig. 15: The motion planning of the manipulator using the method in (Sheng *et al.,* 2006).

$$q_i = a\tan\left(\frac{y_{i+} - y_i}{x_{i+} - x_i}\right) \tag{28}$$

Therefore the manipulability is calculated too. The angles of the links and the manipulability of the manipulator on all the points on the desired path by the proposed method are given in Table 3.

Also, the positions of all the joints by using the method in (Sheng *et al.,* 2006). are given in Tables 4. and 5. From these tables, the angles of the links are calculated for the manipulator on all the points on the desired path. The manipulability on these points is calculated too. The angles of the links and the manipulability of the manipulator on all the points on the desired path are given in Table 6.

Fig. 16. shows the manipulability by using the two methods. From this figure, it should be noted that the proposed method greatly improved the manipulability of the system when compared to the method in (Shibata and Murakami, 2007).

Table 1: the x-axis of all the joints by using the proposed method

	^{x}j1Origin	^{x}j2	^{x}j3	^{x}j4	^{x}j5	^{x}end- effecter
1stpoint on desired path	0	-3.4641	-3.4641	-2.9432.	-1.6932	-0.1611
2nd point on desired path	0	-3.4284	-3.4515	-2.9050	-1.6161	0.1550
3rd point on desired path	0	-3.3602	-3.4284	-2.8341	-1.4435	0.4711
4thpoint on desired path	0	-3.2812	-3.3978	-2.7359	-1.1945	0.7873
5thpoint on desired path	0	-3.2015	-3.3606	-2.6114	-0.8966	1.1034
6th point on desired path	0	-3.1245	-3.3155	-2.4595	-0.5716	1.4195
7thpoint on desired path	0	-3.0511	-3.2608	-2.2786	-0.2334	1.7356
8th point on desired path	0	-2.9818	-3.1944	-2.0683	0.1103	2.0517
9thpoint on desired path	0	-2.9172	-3.1147	-1.8299	0.4554	2.3678
10th point on desired path	0	-2.8583	-3.0206	-1.5662	0.7999	2.6839
Target Point	0	-2.8053	-2.9107	-1.2811	1.1428	3.0000

Table 2: the y-axis of all the joints by using the proposed method

	^{y}j1 Origin	^{y}j2	^{y}j3	^{y}j4	^{y}j5	^{y}end- effecter
1stpoint ondesired path	0	2.0000	5.5000	8.4544	10.6195	11.9051
2nd point on desired path	0	2.0618	5.5680	8.5178	10.6599	11.5890
3rd point on desired path	0	2.1713	5.6768	8.6173	10.6948	11.2728
4thpoint on desired path	0	2.2890	5.7930	8.7190	10.6873	10.9567
5thpoint on desired path	0	2.3993	5.9014	8.8063	10.6255	10.6406
6th point on desired path	0	2.4987	5.9990	8.8743	10.5132	10.3245
7thpoint on desired path	0	2.5879	6.0869	8.9216	10.3593	10.0084
8th point on desired path	0	2.6675	6.1661	8.9468	10.1730	9.6923
9thpoint on desired path	0	2.7379	6.2372	8.9481	9.9617	9.3762
10th point on desired path	0	2.7994	6.3002	8.9241	9.7313	9.0601
Target Point	0	2.8525	6.3553	8.8741	9.4862	8.7440

Table 3: the angles of the links and the manipulability of the manipulator on the points of the desiredpath by the proposed method

	q_1 (rad)	q_2 (rad)	q_3 (rad)	q_4 (rad)	q_5 (rad)	Manipu lability
1st point on desired path	2.6180	1.5708	1.3963	1.0472	0.6981	22.5004
2nd point on desired path	2.6002	1.5774	1.3876	1.0291	0.4831	22.6969
3rdpoint on desired path	2.5679	1.5902	1.3714	0.9809	0.2932	22.7716
4th point on desired path	2.5325	1.6041	1.3483	0.9064	0.1351	22.7906
5th point on desired path	2.4985	1.6162	1.3184	0.8149	0.0076	22.8008
6th point on desired path	2.4670	1.6253	1.2814	0.7149	-0.0945	22.8213
7th point on desired path	2.4382	1.6306	1.2373	0.6127	-0.1764	22.8531
8th point on desired path	2.4118	1.6315	1.1860	0.5126	-0.2427	22.8933
9th point on desired path	2.3879	1.6272	1.1282	0.4174	-0.2971	22.9406
10th point on desired path	2.3666	1.6171	1.0647	0.3288	-0.3422	22.9953
Target Point	2.3478	1.6009	0.9965	0.2473	-0.3802	23.0570

Table 4: the x-axis of all the joints by using the method in [8]

	^{x}j1	^{x}j2	^{x}j3	^{x}j4	^{x}j5	^{x}end- effecter
1stpoint on desired path	0	-3.4641	-3.4641	-2.9432	-1.6932	-0.1611
2nd point on desired path	0	-3.4284	-3.4515	-2.9050	-1.6161	0.1550
3rd point on desired path	0	-3.3534	-3.4274	-2.8321	-1.4478	0.4711
4thpoint on desired path	0	-3.2518	-3.3941	-2.7302	-1.2006	0.7873
5thpoint on desired path	0	-3.1280	-3.3530	-2.6015	-0.8949	1.1034
6th point on desired path	0	-2.9820	-3.3037	-2.4448	-0.5514	1.4195
7thpoint on desired path	0	-2.8093	-3.2449	-2.2573	-0.1868	1.7356
8th point on desired path	0	-2.6013	-3.1750	-2.0366	0.1869	2.0517
9thpoint on desired path	0	-2.3382	-3.0918	-1.7817	0.5622	2.3678
10th point on desired path	0	-1.9437	-2.9934	-1.4940	0.9347	2.6839
Target Point	0	-1.4994	-2.8064	-1.1769	1.3022	3.0000

Table 5: the y-axis of all the joints by using the method in [8]

	^{y}j1 Origin	^{y}j2	^{y}j3	^{y}j4	^{y}j5	^{y}end- effecter
1st point on desired path	0	2.0000	5.5000	8.4544	10.6195	11.9051
2nd point on desired path	0	2.0618	5.5680	8.5178	10.6599	11.5890
3rd point on desired path	0	2.1818	5.6872	8.6275	10.7093	11.2728
4th point ondesired path	0	2.3306	5.8336	8.7592	10.7367	10.9567
5th point on desired path	0	2.4943	5.9927	8.8970	10.7239	10.6406
6th point on desired path	0	2.6673	6.1577	9.0321	10.6647	10.3245
7th point on desired path	0	2.8485	6.3262	9.1590	10.5601	10.0084
8th point on desired path	0	3.0397	6.4968	9.2724	10.4152	9.6923
9th point on desired path	0	3.2463	6.6681	9.3669	10.2364	9.3762
10th point on desired path	0	3.4967	6.8387	9.4372	10.0299	9.0601
Target Point	0	3.7088	6.9579	9.4784	9.8011	8.7440

Table 6: The angles of the links and the manipulability of the manipulator on the points of the desired path by method in [8]

	q_1 (rad)	q_2 (rad)	q_3 (rad)	q_4 (rad)	q_5 (rad)	Manipu lability
1st point on desired path	2.6180	1.5708	1.3963	1.0472	0.6981	22.5004
2nd point on desired path	2.6002	1.5774	1.3876	1.0291	0.4831	22.6969
3rd point on desired path	2.5648	1.5919	1.3710	0.9840	0.2856	22.7530
4th point on desired path	2.5197	1.6114	1.3476	0.9124	0.1102	22.7075
5th point on desired path	2.4684	1.6350	1.3176	0.8194	-0.0417	22.5959
6th point on desired path	2.4118	1.6627	1.2804	0.7116	-0.1709	22.4424
7th point on desired path	2.3493	1.6954	1.2353	0.5949	-0.2794	22.2543
8th point on desired path	2.2786	1.7353	1.1816	0.4747	-0.3698	22.0299
9th point on desired path	2.1950	1.7876	1.1189	0.3552	-0.4446	21.7676
10th point on desired path	2.0781	1.8751	1.0474	0.2394	-0.5062	21.4700
Target Point	1.9550	1.9533	0.9969	0.1294	-0.5569	21.2937

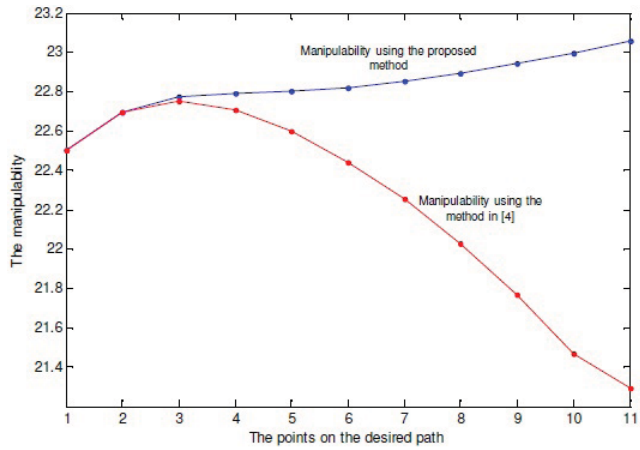

Fig. 16: The manipulability using the proposed method and the method in [8].

Conclusion:

This paper modeled the motion planning of redundant manipulators using a simple geometrical method to find the inverse kinematics of the manipulator. This method can be used for the redundant planar manipulators. The proposed method is compared with the method in (Sheng *et al.,* 2006) and the results show the advantages of this method, because the manipulability using the proposed method is larger than the manipulability using the method in (Sheng *et al.,* 2006). which makes that last link ineffective. A flow chart that can be readily used to solve the redundant motion planning is constructed in this paper. A 5-links redundant manipulator is simulated in this paper.

REFERENCES

Allan de, M., Martins, Anfranserai M. Dias and Pablo J. Alsina, 2006. Comments on Manipulability Measure in Redundant Planar Manipulators. In the Proceedings of IEEE 3rd Latin American Robotics Symposium (LARS '06), pp: 169-173.

Bayraktaroglu, Z.Y., F. Butel, P. Blazevic and V. Pasqui, 1999. A geometrical approach to the trajectory planning of a snake-like mechanism. In the Proceedings of IEEE/RSJ International Conference on Intelligent Robots and Systems (IROS '99), Kyongju, Korea, pp: 1322-1327.

Craig, J.J., 1989. Introduction to Robotics: mechanics and control. 2nd ed. Addison-Wesley Publishing Company Inc.

Damir Omrčen, Leon Žlajpah, and Bojan Nemec, 2007. Compensation of velocity and/or acceleration joint saturation applied to redundant manipulator. Robotics and Autonomous Systems, 55(4): 337-344.

Gianluca Antonelli, 2008 .Stability Analysis for Prioritized Closed-Loop Inverse Kinematic Algorithms for Redundant Robotic Systems. In the proceedings of IEEE International Conference on Robotics and Automation (ICRA 2008), pp: 1993-1998.

Kircanski, M.V. and T.M. Petrovic, 1991. Inverse Kinematic Solution for a 7 dof Robot with Minimal Computational Complexity and Singularity Avoidance. In the Proceedings of IEEE International Conference on Robotics and Automation, Sacramento, California, USA, 3: 2664-2669.

Lee, C.S.G. and M. Ziegler, 1984. Geometric Approach in Solving Inverse Kinematics of PUMA Robots. IEEE Transactions on Aerospace and Electronic Systems, AES-20(6): 695-706.

Maria da, M., B.M. Graça, D. Fernando, J.A. Tenreiro Machado, 2008. Fractional dynamics in the trajectory control of redundant manipulators. Communications in Nonlinear Science and Numerical Simulation, 13(9): 1836-1844.

Mittal, R.K. and I.J. Nagrath, 2007. Robotics and control. New Delhi: Tata McGraw-Hill.

Naoyuki Kubota, Takemasa Arakawa and Toshio Fukada, 1998. Motion Learning for Redundant Manipulator with Structured Intelligence. In the Proceedings of the 24th Annual Conference of the IEEE Industrial Electronics Society (IECON '98), 1: 104 – 109.

Nearchou, 1998. Solving the inverse kinematics problem of redundant robots operating in complex environments via a modified genetic algorithm. Mechanism and Machine Theory, 33(3): 273-292.

Robin, R., Murphy, Introduction to AI Robotics, 2000. A Bradford Book. The MIT Press, Cambridge, Massachusetts, London, England.

Shibata, T. and T. Murakami, 2007. A Null Space Force Control Based on Passivity in Redundant Manipulator. In the Proceedings of IEEE International Conference on Mechatronics, Kumamoto, Japan, pp: 1-6.

Sheng, L., W. Yiqing, C. Qingwei and H. Weili, 2006. A new Geometrical Method for the Inverse Kinematics of the Hyper-Redundant Manipulators. In the Proceedings of IEEE International Conference on Robotics and Biomimetics (ROBIO '06), Kunming, China, pp: 1356-1359.

Perez, A. and J.M. McCarthy, 2005. Sizing a Serial Chain to Fit a Task Trajectory Using Clifford Algebra Exponentials. In the Proceedings of IEEE International Conference on Robotics and Automation (ICRA 2005), Barcelona, Spain, pp: 4709-47 15.

Xia, and J. Wang, 2001. A dual neural network for kinematic control of redundant robot manipulators. IEEE Transactions on Systems, Man, and Cybernetics, 31(1): 147–154. A. C.

Yoshikawa, T., 1985. Manipulability and redundancy control of robotic mechanisms. In the Proceedings of IEEE International Conference on Robotics and Automation, pp: 1004-1009.